Influence of processing conditions on manufacturing polyamide parts by ultrasonic molding

J. Grabalosa [a,*], I. Ferrer [a], A. Elías-Zúñiga [b], J. Ciurana [a]

[a] Department of Mechanical Engineering and Industrial Construction, Universitat de Girona, Av/Lluís Santaló s/n, Girona 17003, Spain
[b] Centro de Innovación en Diseño y Tecnología, Department of Mechanical Engineering, ITESM, Campus Monterrey, 64849, Mexico

a b s t r a c t

Ultrasonic molding is a new manufacturing process for producing small and micro polymeric components wherethe material is plasticized using vibration energy. In small parts manufacturing, replicability is usually demanded. Downscaled tensile specimens were manufactured using ultrasonic molding on polyamide pellets not only to ob- tain specimens, but also to investigate the influence of the processing conditions on process performance and material characterization. A modeling approach is proposed to assess the energy flow involved in the process. It was observed that 300 mg of polyamide could be plasticized and injected in less than 3 s and the results showed a relationship between the processing conditions and the final product, i.e. the higher the values of applied pres- sure, ultrasonic time and vibration amplitude, the more accurate and more homogeneous parts were. Moreover, the material did not suffer chemical degradation, but light variation on the molecular weight and different chainalignment along the specimen were detected. The mechanical properties measured were slightly influenced bythe processing conditions and were in accordance with what would be expected for that particular material when being processed using conventional injection molding.

1. Introduction

Product miniaturization is, nowadays, a consistent trend in industrial sectors where devices are becoming smaller and have more complex geometries. Some sectors experiencing an increase in this demand for micro products are information technology (IT) sector, the biomedical sector, the automotive industry, telecommunications and aerospace [1]. In some cases, these components have to be manufactured using sophisticated materials, which not only increases production costs, but also complicates the manufacturing process (e.g. reinforced materials or medical devices), resulting in cost per unit increases, especially if small series of these products are demanded.

Micro-injection molding (μIM) is a key technology for the mass-production of polymeric parts with micro-features [2,3]. Replicability, repeatability and high precision are guaranteed in this process. However, other processes such as hot embossing, reaction injection molding, injection compression molding, thermoforming or extrusion are also used to produce thermoplastic micro parts [4]. Now, a new technology called ultrasonic molding has appeared.

Ultrasonic molding is an innovative manufacturing process, which produces polymeric micro parts where the material is melted by the energy applied by ultrasonic vibration. This energy produces the polymer plasticization mainly via two mechanisms [5]: (i) the internal friction of the material, which is a factor related to material damping properties and (ii) the friction caused by the relative movement between the pellets. This combination increases the local temperature until the polymer melts.

The material is firstly placed in the plasticization chamber in the mold in solid pellet form. Then, the process starts and the sonotrode, which is the element that delivers the ultrasonic vibration to the material [6], starts to move until it reaches the material (Fig. 1a). At this point, it begins to vibrate as it continues its movement, causing the material to melt. Here, the sonotrode also acts as a plunger and forces the molten material to flow through the runners and fill the mold cavity. At the same time as the material melts, it is introduced into the mold cavity by the downward movement of the sonotrode. When the ultrasonic vibration stops, the sonotrode continues applying pressure to the material in order to pack it during the cooling stage (Fig. 1b). Finally, the sonotrode returns to its initial position, and the mold can be opened to extract the final part. Depending on the diameter of the sonotrode, the dimensions of the plasticization chamber and the power of the ultrasonic equipment, the amount of material that can be processed varies.

Ultrasound has been successfully used in the welding and riveting of polymeric components to produce neat bonding in a short time [7]. Ultrasonic energy is rapidly dissipated within the polymer causing local melting in the contact area. Taking advantage of this phenomenon,

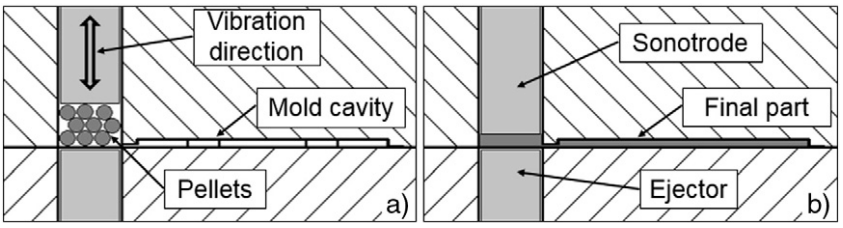

Fig. 1. Ultrasonic molding process representation: a) Start of the cycle, b) End of the cycle.

Michaeli et al. [7] proposed the use of ultrasonic energy to improve the plasticizing efficiency in micro injection molding processes. A very small amount of material was plasticized in an ultrasonic prototype set, thus obtaining a homogeneous material structure. Later, Michaeli and Opfermann [8] adapted the acoustic unit and the mold cavity of a conventional ultrasonic welding press to study the potential of ultrasonic plasticization. From preliminary experiments, they found that less than 3 s were needed to melt 500 mg of polyoxymethylene (POM) and obtain a homogeneous structure. Moreover, they found a relationship between vibration amplitude and plasticizing time, which would avoid polymer degradation. Next, instead of pellets they used disc shapes taken from a plastic sheet as rough material and the melt generated during the plasticizing process was pushed by the sonotrode into a mold cavity of micro-disc shapes. The part quality was poor due to the low injection pressure and the missing holding pressure in the set-up developed. Afterwards, Michaeli and Kamps [9] analyzed the effect of vibration amplitude and ultrasonic time on the amount of energy applied to the polymer. They recorded a temperature distribution along the lateral surface of a 2 mm solid polycarbonate (PC) cylinder in order to avoid the effect of pellet friction. They found that by using higher amplitudes, higher heating rates were achieved, and they were able to reach maximum values of 800 °C/s of material heating. Later on, Michaeli et al. [5] studied the ability of ultrasonic energy to process micro parts using different materials (polypropylene (PP) and POM), and the effect of the process parameters on the weight and the morphology of the resulting parts. They found that the vibration amplitude and compression force had little effect on the weight of the part, whereas the amplitude did affect the molten material. This was established with microscope images that revealed the presence non-molten parts when lower energy was applied. Flow lines were observed in PP specimens, probably caused by a melting temperature being reached that was too low. Jiang et al. [10] studied the effect of ultrasonic voltage and pressure on the plasticization speed of the polymer and observed that for higher values of those parameters, higher plasticization speed was obtained. The ultrasonic voltage determines the amount of energy supplied to the material, resulting in higher plasticization speed. However, pressure influence was weak due to the reduction of ultrasonic cavitation effect, reducing the amount of bubbles formed in the liquid, caused by pressure variations, which then collapses and releases heat energy. Recently, in 2014, Sacristán et al. [11] used ultrasonic energy to produce polylactide (PLA) samples. Varying vibration amplitude and applied pressure, they found that higher levels of both parameters lead to material degradation, while samples presented material inhomogeneity when lower values were set. A relationship between the processing parameters was required to obtain homogeneous specimens. Planellas et al. [12] produced PLA and polybutylene succinate (PBS) micro parts by means of ultrasonic molding, and they found that there was no significant molecular degradation when the process parameters (ultrasonic time, amplitude and injection force) were optimized. Negre et al. [13] presented a study of the effect of the melting velocity and vibration time over part weight and dimensions. They found that three seconds of vibration energy were necessary to melt and inject 0.3 g of PP. A variation of porosity and homogeneity along the specimen were detected.

In reality, little research has been carried out on this technology, and most of it provides general views about the effect of the main process parameters, such as pressure or amplitude, on the plasticizing process and polymer temperature. However, as an emerging technology, ultrasonic molding faces many challenges such as difficulties in microcavity filling, dimensional accuracy, mechanical properties characterization, and microstructure analysis of micro products. The aim of this paper is to provide a preliminary study of the influence of the process parameters of ultrasonic molding on the part filling, dimensional accuracy and mechanical properties, not yet researched in the literature. Moreover, the homogeneity of the parts obtained and the polymer degradation were evaluated using different techniques. Finally, an energy balance, which considers the theoretical dissipated energy, the energy provided by the process, and the energy required to melt the material, is proposed. The biomedical material, polyamide (PA12), was used in this study.

2. Mathematical modeling of the ultrasonic energy balance

The mathematical modeling approach proposed in this investigation is based on the fundamentals of acoustic/ultrasound energy. In terms of the process, it is considered the dissipated energy resulting from oscillation movement and the movement of the sonotrode. Whereas, in terms of the material, the theoretical melting energy required is also included.

According to Rienstra and Hirschberg [14], the equation that describes the acoustic energy of a homentropic flow is given as:

$$\frac{\partial}{\partial}\left(\rho e + \frac{1}{2}\rho v^2 + \nabla \cdot \left(v\left(\rho e + \frac{1}{2}\rho v^2 + p\right)\right.\right.$$
$$= -\nabla \cdot q + \nabla \cdot (\tau \cdot v) + f \cdot v; \qquad (1)$$

where ρ is the density of material, e is the internal energy per unit mass, q is the heat flux resulting from the heat conduction, v is the material's flow velocity, f is the external force density, p is the pressure, τ is the viscous stress tensor, and ∇ is the symbol representing the gradient operator. The q flux comes from the viscous effects of the material and becomes important because the pulsation of the applied sonotrode load is related to the resistance entanglement molecular forces [15,16] and has physical and chemical effects on the polymer melt that influence the apparent polymer viscosity and the melt molecular weight, respectively [17]. Furthermore, applying acoustic energy to a polymeric material produces a melt that is considered a non-Newtonian fluid [18] and then the density fluctuations in the material are assumed to be small [14]. Thus, the total polymeric melt energy density is given as:

$$E_{tot} = \rho e + \frac{1}{2}\rho v^2 : \qquad (2)$$

When the ultrasonic energy propagates in the fluid thorough oscillatory waves, the vibration energy per unit area is known as the fluid energy flux intensity, which is given as:

$$I_{tot} = v\left(\rho e + \frac{1}{2}\rho v^2 + p\right) : \qquad (3)$$

Since this energy flux propagates in the vertical sonotrode direction then, the flux intensity can be estimated from the relationship [16]

$$I = 2\pi^2 \rho c f^2 x^2 = A f^2 x^2; \quad (4)$$

where f is the driving frequency of the ultrasonic vibration, and x is the mean vibration amplitude. In our system, the value of $f = 30$ kHz. It is well known that if the ultrasound flux intensity has a large magnitude this could lead to a faster rate of chain scission in the polymer melt [19] and then, the energy flux intensity I is partially consumed by a chain resistance force, which is directly related to the polymer melt shear stress. Therefore, Eq. (4) can be re-written as:

$$I = A f^2 x^2 = E_k' \int F dx; \quad (5)$$

where E_k' is the vibration energy, and F is the resistance force related to the shear stresses responsible for the polymer chain scission [20]. The shear effects as a function of the polymer viscosity and molecular weight have been widely discussed [21,22], but it is out of the scope of the present article.

2.1. Material dissipated energy density

Based on the ultrasound injection process illustrated in Fig. 1, it is expected that the dissipation energy derived from the material during the injection process, must be determined from the oscillatory amplitudes provided by the sonotrode. From a sinusoidal vibrations amplitude distribution, the material experienced varying stresses and strains that are related to its energy consumption [10]. The equations that defined the sinusoidal stress and strain in the polymeric materials are given as:

$$\sigma = \sigma_0 e^{i\omega t}; \quad (6)$$

$$\varepsilon = \varepsilon_0 e^{i\omega t}; \quad (7)$$

where σ and ε are the stress and strain, respectively, Ω represents the sonotrode angular frequency ($\Omega = 2\pi f$), and, by definition, $i = \sqrt{-1}$: Here σ_0 and ε_0 are, respectively, the maximum stress and strain at which polymer chains scission start [19]. By assuming that our material has viscoelastic behavior then, the expression that relates these two parameters is assumed to be given by:

$$\sigma_0 = \varepsilon_0 G \sin(\omega t + \delta); \quad (8)$$

whose trigonometrical expansion provides:

$$\sigma_0 = \varepsilon_0 (G \cos\delta) \sin\omega t + \varepsilon_0 (G \sin\delta) \cos\omega t \equiv \varepsilon_0 G' \sin\omega t + \varepsilon_0 G'' \cos\omega t; \quad (9)$$

where G is the elastic modulus, G'' is the viscous modulus, and the phase angle δ, which describes the phase difference between the dynamic stress and the dynamic strain, can be determined from the loss factor relationship

$$\tan\delta = \frac{G''}{G'} \quad (10)$$

when performing experimental dynamic mechanical analysis (DMA) tests. Thus, the total energy density per cycle can be calculated from:

$$W = \int_0^{2\pi/\omega} \sigma \frac{d\varepsilon}{dt} dt = \int_0^{2\pi/\omega} G'\varepsilon \sin\omega t(\varepsilon_0 \omega \cos\omega t) dt + \int_0^{2\pi/\omega} G''\varepsilon (\cos\omega t)(\varepsilon \omega \cos\omega t) dt = \pi\sigma_0\varepsilon_0 \sin\delta \quad (11)$$

from which the average energy density dissipated per cycle could be determined from the expression

$$Q_{avg} = \frac{\pi\sigma_0\varepsilon_0 \sin\delta}{2\pi/\omega} = \frac{\sigma_0\varepsilon_0\omega \sin\delta}{2}. \quad (12)$$

2.2. Ultrasound injection process: dissipating energy

The ultrasonic energy applied by the sonotrode to the pellets, results in an increase in temperature that melts the material and then this material fills a mold cavity. In an attempt to theoretically describe the dissipated energy within the material per cycle, we assume that the power generated could be described by the equation:

$$P = \frac{dW}{dt} = Fv_{avg}; \quad (13)$$

where F is the applied sonotrode force and v_{avg} is the average acoustic vibration velocity [23] that can be determined from the equation that describes the acoustic oscillations that the sonotrode tip experiences:

$$x(t) = a \sin(2\pi\omega t): \quad (14)$$

Here Ω is the ultrasonic frequency and a is the oscillatory amplitude of the sonotrode tip. Thus, the generated power is given as:

$$P = Fv_{avg} = 4pAa\omega; \quad (15)$$

then, the dissipated heat flux during the ultrasound injection process could be found from the following expression:

$$q = \frac{P}{dV_g} = 4pa\omega \quad (16)$$

where A is the sonotrode area.

2.3. Material melting energy

The energy required to melt the material can be estimated using basic thermodynamic equations. Considering the amount of material that is melted in each cycle, (the heat capacity of the material and the fusion heat) as well as the temperature increase required to reach the material's melting temperature, an approach of the minimum energy required can be obtained using the following equation:

$$Q_m = mC_P\Delta T + m\Delta H_f \quad (17)$$

where C_p is a heat constant, ΔT is the temperature difference, and ΔH_f represents the enthalpy of fusion.

3. Experimental procedure

3.1. Machine and process parameters

An adapted ultrasonic welding pneumatic press with a 1500 W ultrasonic generator was used to carry out the experimentation (Fig. 2). The whole acoustic configuration (the transducer, the booster and the sonotrode) provided 35 μm of vibration amplitude at a frequency of 30,000 Hz at the tip of the sonotrode. The sonotrode has a lineal vertical movement and is the key element that transmits ultrasonic vibration to the polymer pellets to be melted. Its movement is governed by the pressure applied by the pneumatic piston, which results in different force and speed magnitudes of the sonotrode. Consequently, the total amount of energy supplied by the generator to the material in each cycle may vary according to the processing conditions and the material being considered. The variation in the supplied energy is automatically controlled and cannot be adjusted in this machine's configuration. The mold is assembled below the acoustic unit.

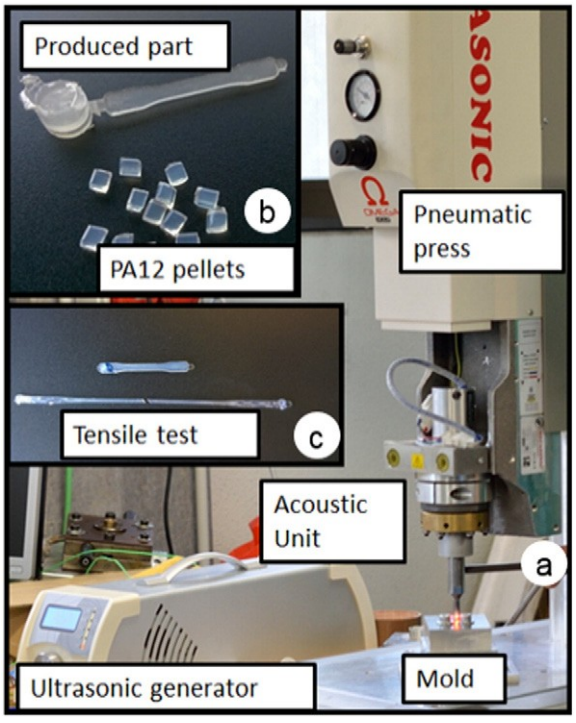

Fig. 2. Experimental setup: a) Ultrasonic molding equipment, b) Raw material and final part and c) Tensile tests.

The process parameters able to be controlled are: ultrasonic time, vibration amplitude and pressure applied, and the setting temperature of the mold. The ultrasonic time represents the vibration time of the sonotrode. Vibration amplitude is the maximum displacement at the tip of the sonotrode and can be adjusted by increments of 10%. Finally, the pressure transmitted to the acoustic unit produces the sonotrode movement and determines the force at the tip of the sonotrode. One bar measured by the manometer represents 311 N of force at the tip of the sonotrode, resulting in a theoretical pressure in the plasticization chamber of around 6 MPa. The temperature of the mold was fixed at room temperature [23.5 °C] in accordance with the material's datasheet recommendations for injection molding. Melting temperature cannot be controlled in this technology because the melting process occurs inside the mold and the material is injected directly into the cavity.

3.2. Material and part geometry

Medical grade natural polyamide (Rilsamid™ PA 12 G AMNO TLD) pellets characterized by their excellent resistance to chemicals, high dimensional stability and ease of processing (see properties in Table 1) were used in this study. According to the material's datasheet, the melting temperature is 178 °C and the recommended injection conditions are an injection temperature range of 230–290 °C and a mold temperature between 20 and 40 °C. Drying for 4–6 h at 80–90 °C is recommended.

Table 1
PA12 material properties.

Property	Value
Density [kg/m^3]	1020
Melting point [°C]	178
Glass transition temperature [°C]	41
Melt volume index [cm^3/10 min]	57
Shrinkage [%]	0.8
Tensile stress at yield [MPa]	38
Tensile strain at yield [%]	7
Young's modulus [GPa]	1.8

A tensile bar geometry was used in this experimentation and its dimensions were decided in accordance with ASTM D638 standards. Considering the limitation on the amount of material to be processed for each cycle, dimensions were scaled at 1:5. The geometry and final dimensions of the parts obtained are shown in Fig. 3a. The connection between the mold cavity and the plasticization chamber is made by a simple direct gate with a 2 mm wide, 0.4 mm high rectangular section, and a 2 mm long runner. As shown in Fig. 3b, the sprue includes a cylindrical shape caused by plasticization chamber geometry, which is needed to transmit the pressure from the sonotrode to the molten material. The injection, center and end region of the sample were examined to assess material degradation and alignment.

The mold was manufactured using AA6061-T6 aluminum alloy, which is a commonly used material in the mold industry, supplied by Broncesval S.L. Its dimensions were checked using a coordinate-measuring machine. The dimensions of the central part of the mold were 2.493 mm wide and 1.247 mm thick.

3.3. Experimental design

Experimentation was divided into two steps: a screening phase and the experimental plan. In the screening phase, upper and lower limits for the parameters tested were established. The pressure applied, the ultrasonic time and the vibration amplitude were studied. Each parameter was varied independently, while keeping the others constant, from the minimum until the maximum allowed values, and which were determined according to workshop facilities and equipment performance. Table 2 summarizes the levels tested for each parameter and the corresponding fixed values. The pressure applied was varied from 0.5 to 5 bar, vibration amplitude was reduced from the maximum amplitude obtained in steps of 10% and vibration time was varied from 0.5 to 6 s. As the maximum power generated cannot be varied in this machine it was kept constant at 1500 W.

Once the maximum variation range was established, a more accurate design of experiments was carried out in the experimental plan to investigate the effect of the process parameters on filling quality and the polymer characterization after being processed.

3.4. Part characterization

Filling quality is assessed in four ways: part filling ratio, dimensional accuracy, part homogeneity and mechanical properties. The part filling ratio is the percentage of the measured completed part when comparing the flow length obtained in regards to the total specimen length. Dimensional accuracy is analyzed in the central zone of the tensile bar by measuring the width and thickness to determine the influence of the processing conditions in terms of molding accuracy and material shrinkage. As shown in Fig. 3a, three different measures for width (w_i) and thickness (t_i) were made using a digital micrometre (Micromar 40 EWV). Those dimensions are the most important in tensile specimens, because this is the part section where the sample breaks and thus is used to calculate the mechanical properties. The mechanical proprieties of completed parts were tested in an MTS Insight testing machine. In accordance with ASTM 638 standards a 1 kN load cell was used to test the specimens at a constant speed of 50 mm/min until breaking point. Tests were performed at room temperature (23.5 °C) and a relative humidity of 50%.

In order to study the degradation mechanism of the manufactured polymer samples, three different experimental techniques were used for the samples characterization: Fourier Transform Infrared Spectroscopy (FTIR), Gel Permeation Chromatography (GPC), and small/wide angle X-ray scattering (SWAXS). FTIR analysis were performed at a resolution of 4 cm^{-1} using a Shimadzu spectrometer. Three different sections of specimens processed with different vibration times were

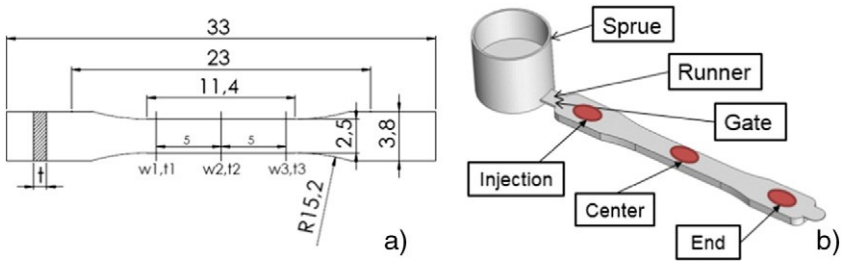

Fig. 3. a) Tensile specimen dimensions in mm (t = 1.25 mm thickness), and b) Part and sprue obtained after molding with the characterization zones.

analyzed in order to assess chemical degradation of the ultrasonic polymer processing. Molecular weight of raw material and three different zones of a specimen was measured using Alliance 2695 GPC equipment coupled to a Waters 2998 UV-Vis detector to observe and measure molecular weight distribution and variation along the parts. SWAXS patterns at 0° and 90° at three different regions of the same specimen were analyzed to address the polymer chain alignment. Finally, parts were examined using a Nikon SMZ-745T microscope.

4. Results and discussion

The screening experiments demonstrated that vibration amplitude strongly affects cavity filling. Upon decreasing the value of this parameter, the number of completed specimens obtained was drastically reduced. For instance, with 80% amplitude, less than 15% of completed specimens were obtained and no repeatability was observed. In fact, some of the samples presented solid pellets in the plasticization chamber, which means that the applied energy when the amplitude was reduced is not enough to completely melt the material. With ultrasonic time, about 1 s was necessary to obtain enough polymer melt to start filling the cavity. When ultrasonic energy was applied for more than 5 s, polymer degradation was observed in the area where the sonotrode was in contact with the polymer, inside the plasticizing chamber. In the case of pressure applied, values lower than 2 bar resulted in incomplete specimens, while 90% of completed parts were obtained when using pressure higher than 2 bar. When pressure was higher than 5 bar, the acoustic equipment overloaded because as a result the excess of force between the sonotrode and the material the vibration frequency went out of range and this interrupted the molding cycle.

Based on these previous results, a full factorial design of the experiments' methods was used to study the effect of the more relevant process parameters, ultrasonic time and the pressure applied, on the filling quality. A total of 20 different combinations were tested with 5 experiments for each level, resulting in 100 different experiments. The vibration amplitude was maintained at the maximum for the acoustic unit configuration (35 μm), the cooling time at 2 s and the mold temperature at 25 °C. PA12 pellets were dried at 90 °C for more than 4 h.

Experimental results are summarized in Table 3. The mean values of part filling, dimensional accuracy and mechanical properties are presented. Dimensions and mechanical properties were only measured when completed parts were obtained.

Table 2
Screening phase experiments.

Process parameters	Screening phase		
	Experiment 1	Experiment 2	Experiment 3
Pressure (bar)	[0.5–5]	3	3
Vibration time (s)	3	3	[0.5–6]
Amplitude (μm)	35	[3.5–35]	35

4.1. Part filling ratio

The part filling ratio is defined as the flow length divided by the expected specimen length. The mean value and the standard deviation are presented in Table 3. It was observed that a minimum of 2 s of ultrasonic time is required to obtain completed parts (more than 95% filling ratio). In terms of pressure, 2 bar or higher was needed to obtain full specimens. Nevertheless, results evidence the interdependence between both process parameters. To obtain completed specimens with 2 s of ultrasonic energy, the material had to be pushed with the highest pressure (4 bar), while higher values of ultrasonic time (a minimum of 3 s) were needed for lower values of pressure applied (2 bar). For this reason, it is interesting to plot the filling ratio as a function of both parameters (Fig. 4) to identify the expected value of cavity filling for each combination of ultrasonic time and pressure applied. In this contour map each color represents a 10% reduction of the filling, from red (representing 90% of the filling cavity) to blue (representing 10% of the filling cavity). The region bounded by a dotted line corresponds to experiments that produced completed parts.

In fact, as evidenced in Fig. 4, a minimum of 2 s of ultrasound and a pressure of 2 bar are required to obtain completed parts, and when these parameters are increased, the flow length is also increased. Moreover, it also reveals the relationship between both parameters, because for lower values of pressure applied, greater ultrasonic times are required, and vice versa.

A two-way analysis of variance (ANOVA) was performed in order to observe and compare the effect of the two different and independent varied factors (vibration time and pressure applied) as well as the interaction between the parameters on cavity filling. The interaction between the parameters and the main effects plot for cavity filling, considering the filling percentage as a response, and the ultrasonic time and pressure applied as factors are presented in Fig. 5. Both parameters were found to be influencing forces.

Fig. 5a evidences that the length of time ultrasound is applied has a considerable influence on ultrasonic molding. By increasing the vibration time, more ultrasonic energy is applied to the material. Therefore, more material is melted and the average temperature increases, reducing the material's viscosity and facilitating mold filling. However, applied to prevent polymer degradation, which was detected in the material in contact with the sonotrode for ultrasonic time higher than 5 s, the amount of energy applied has to be controlled.

Fig. 5a reveals a positive effect of the pressure applied. As expected, increments of the pressure applied increased filling ratio, because the molten material is pushed faster into the mold cavity. Consequently, although the material is at the same temperature, further zones can be achieved before the material freezes. Moreover, the pressure applied can also affect the friction heat generated in ultrasonic molding, producing higher melt volume at the same vibration times.

In Fig. 5b, the main effects plot for both processing parameters is presented. The effects of the pressure applied and ultrasonic time are greater when the lowest levels were used, because the slopes are higher, especially for the ultrasonic time. On comparing both parameters, the influence of ultrasonic time is higher than that of pressure. However,

Table 3
Experimental plan results: part filling, samples dimensions and mechanical properties.

Process parameters			Part filling ratio		Dimensions		Mechanical properties		
Amplitude (μm)	Vibration time (s)	Pressure (bar)	Mean (%)	SD (mm)	Width (mm)	Thickness (mm)	Stress (MPa)	Strain (%)	E modulus (GPa)
35	1	1	0	0					
		2	0	0					
		3	7.07	1.15					
		4	13.13	0.58					
	2	1	24.24	2.65					
		2	51.52	5.96					
		3	80.61	3.21					
		4	99.39	0.45	2.479	1.235	36.10	11.35	1.31
	3	1	55.15	2.17					
		2	100	0	2.481	1.240	36.30	10.91	1.38
		3	98.79	0.89	2.477	1.240	35.20	10.15	1.35
		4	98.18	1.34	2.482	1.241	36.10	10.30	1.39
	4	1	76.97	0.89					
		2	100	0	2.483	1.243	36.45	10.44	1.43
		3	98.79	0.89	2.482	1.243	36.50	10.44	1.41
		4	100	0	2.484	1.244	36.60	10.60	1.38
	5	1	72.12	2.77					
		2	100	0	2.481	1.244	37.20	10.76	1.42
		3	98.18	1.34	2.482	1.245	36.85	10.76	1.36
		4	97.58	1.79	2.481	1.245	36.95	10.44	1.40

from 3 s onwards, this effect is reduced, and no effect on cavity filling is obtained when ultrasound time is increased from 4 to 5 s. This is because, after 4 s the mold has either already been filled, or the material inside the mold has already solidified. Therefore, no more molten material can be introduced inside the mold and all the energy is applied material allocated in the plasticization chamber, causing material degradation.

4.2. Part dimensions

The dimensions of the central section of the tensile specimens were measured for each combination of processing conditions. The average width (w_1, w_2, w_3) and thickness (t_1, t_2, t_3) measurements are presented in Table 3.

Fig. 6 contains the dimensions box plot as a function of the processing parameters. Considering all the values, there is a variation range of 22 μm in the case of thickness, and 39 μm for width. Dotted lines correspond with the mold cavity real dimensions. In general, better accuracy is obtained in the case of thickness, almost achieving the target value in some processing conditions.

Fig. 6a reveals that thickness accuracy improves when the pressure applied and amount of ultrasound time increase, thus obtaining thicker specimens when both parameters were at their maximum. The difference between the target value and mean thickness value is between 2 and 12 μm, which represents a dimensional accuracy of 99.87% in the best conditions (5 s of ultrasound and 4 bar) and 99.11% in the worst cases (2 s of ultrasound and 4 bar of pressure).

Width dimension is plotted in Fig. 6b, and results do not show any clear trend under the different processing conditions. The mean value of width has a variation range of 22–29 μm deviation from the target value, leading to an accuracy from 98.86% to 99.05%.

The improvement in precision with pressure and ultrasonic time, (clearly observed in the case of thickness), was expected because an increment of each factor results in more energy being applied to the polymer. Thus, if material is introduced at a higher temperature, material viscosity is reduced, and the mold is easily filled. Moreover, it starts to freeze later. Furthermore, if the applied pressure is higher, the flow rate is incremented, the mold is filled faster and packing pressure acts when material temperature is higher, resulting in better accuracy. This increase in dimensional accuracy as a function of melt pressure is also observed in conventional injection molding [24].

The differences between the accuracy in thickness and width is due to the rectangular section studied, in which width dimension is two times larger than thickness. This longer dimension has greater contact surface where the material solidifies earlier, thus reducing the packing pressure effect and affecting replication accuracy.

In fact, the injection pressure values in ultrasonic molding (30 MPa) are very low compared to those applied in microinjection processes (160–350 MPa) [25]. However, as the results here showed, cavity filling with good accuracy is guaranteed with this technology, because

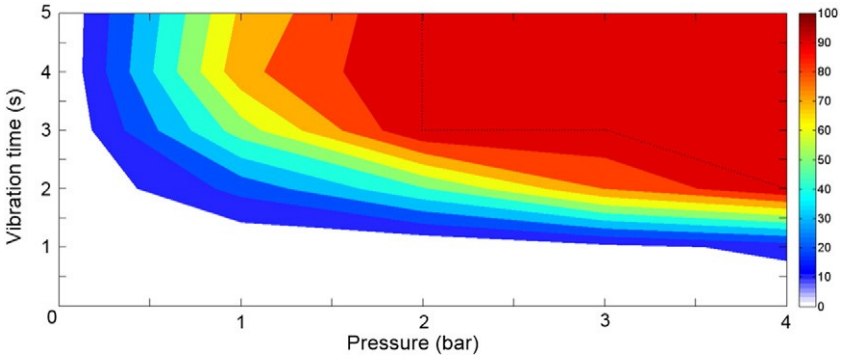

Fig. 4. Process windows for PA12 specimens. With dotted line, the region depicting the combination of the processing conditions producing completed specimens.

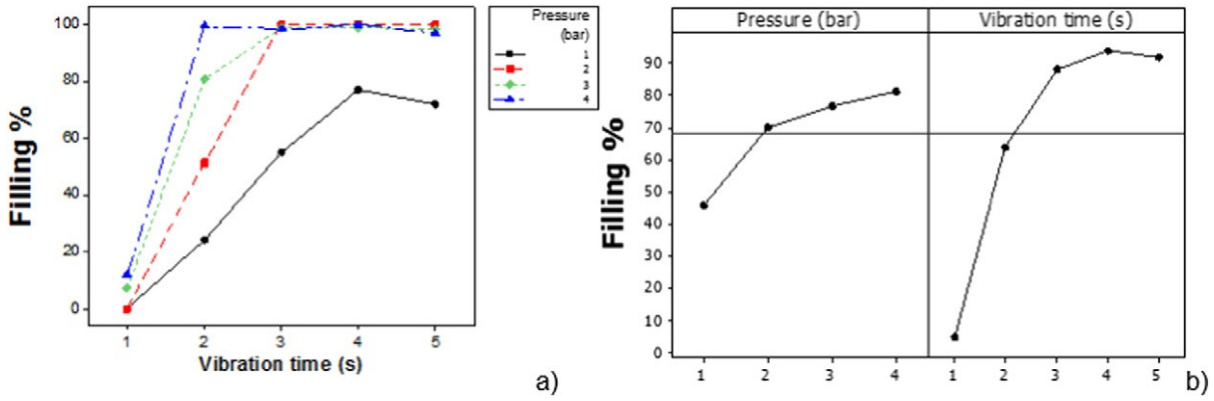

Fig. 5. Effect of processing conditions on cavity filling: a) Interaction between parameters and b) Main effects plot.

ultrasonic waves are applied directly to the material near the entry of the mold and this acoustic energy is propagated along the melt to reduce its viscosity and increase filling efficiency.

Analyzing the cycle time in in ultrasonic molding technology, it is less than 10 s, including mold movement, the melting process and cavity filling. Although the shot time can be faster in microinjection processes, the polymer takes much more time in the heated barrel where it is melted, which is usually not included in the cycle time calculations. This demonstrates the relevance of ultrasonic molding technology when small and medium batches have to be produced.

4.3. Mechanical properties

The material properties of the parts manufactured via ultrasonic molding were measured. Two specimens from each set of experiments that produced complete tensile bars were mechanically tested. Experimental results are presented in Fig. 7.

In Fig. 7, it can be observed that specimens manufactured with the different processing conditions behave similarly in the tension tests. Stress – strain curves indicate that the yield point is reached at similar values with low variation. The variation of the yield strength is lower than 5%, which can be caused by experimentation variability. However, in the enlarged image of the yield point (Fig. 7a), it can be observed that material behavior is somewhat influenced by the processing conditions. In general, samples processed at longer ultrasonic time, which are plotted in different colors, presented higher values of yield strength, while changes in applied pressure (different line style) do not present any significant influence. The stress values obtained, presented in Table 3, varies 1.7 MPa between samples produced with different processing conditions (35.5–37.2 MPa), while strain values changed between 10.1% and 11.4%, with a total variation of 1.3%.

The analysis of Young's modulus obtained from the first zone of the strain – stress curve (Fig. 7b) evidences little influence regarding the processing time. The stiffness of samples processed with 2 s of ultrasound (green curves) is clearly lower, with an obtained value of 1.31 GPa. Other experiments had similar performances, but higher slope on the curve was detected when ultrasonic time was increased, with obtained values around 1.40 GPa. In any case, the expected value of 1.8 GPa is achieved.

Polyamides are slow crystallizing polymers, which means that, as a semi-crystalline material, their structure should be modified depending on the cooling of the sample. Therefore, varying the amount of energy applied to the material, melt temperature and flow rate might differ between tests, which would, in turn, lead to different cooling rate. Consequently, samples should present different crystalline structures which will affect the material's properties.

Comparing these results to the PA12 raw material datasheet (38 MPa and 7% of elongation at the yield point), some differences were detected. The values of stress at the yield point were slightly lower than the values reported in the raw material data sheet (4% lower) and the values of strain observed were greater than those documented in the raw material properties, being around 10.5% of elongation in comparison to the 7% expected. However, the melting mechanism in ultrasonic molding is different to conventional injection molding, where the material is melted by heat, and this should affect the final material performance. Then, mold design, including gates and runners, do influence part filling and final mechanical properties [26]. Finally, according to Meister and Drummer [27], downscaled tensile bars of polyamide obtained by injection molding present lower stiffness and strength while the strain at break was increased as a result of its modified crystalline structure. Considering their results, yield strength is 90% and Young's modulus is around 70%. In this regard, the results

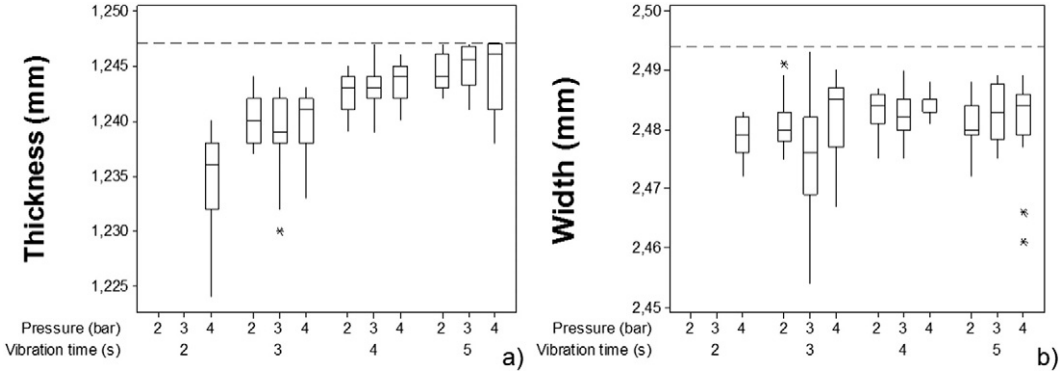

Fig. 6. Effect of processing conditions on dimensional accuracy: a) Thickness and b) Width.

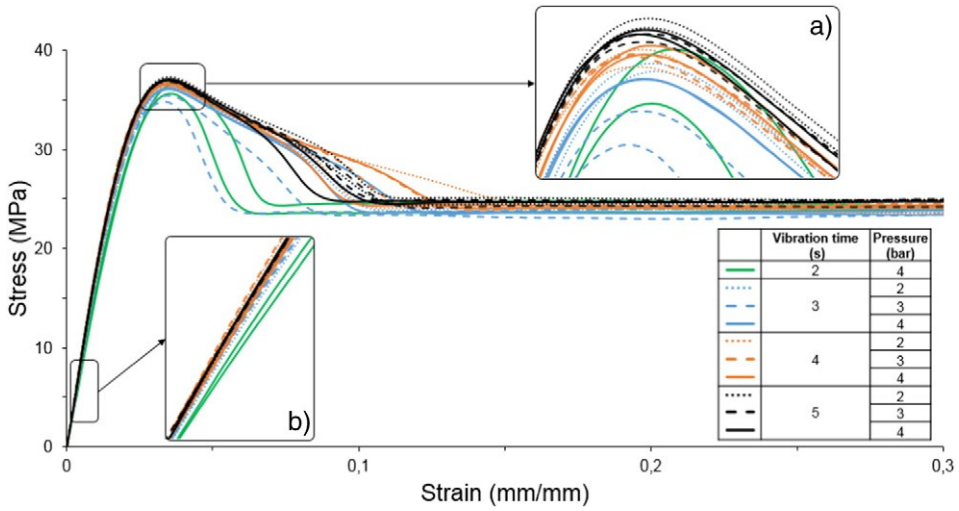

Fig. 7. Experimental results of tension tests from PA12 samples processed by ultrasonic molding.

obtained are in accordance with the reported properties for injection molding.

4.4. Material characterization

Fig. 8a presents the comparison of the obtained FTIR spectra of parts processed at different vibration time with the original raw material. Fig. 8b shows the FTIR spectra comparison at the injection, center and end region of the specimen processed at 4 bar and 5 s of vibration. The characteristic peaks of polyamides corresponding to the – NH group of PA12 are located at 3294 cm^{-1} (stretching vibration) and 1553 cm^{-1} (bending vibration), respectively. The peaks at 2848 and 2918 cm^{-1} belong to the symmetric and asymmetric stretching vibration modes of CH2, respectively. The peaks at 721 and 1465 cm^{-1} are attributed to CH2 groups of the polymer. The FTIR results show that there is no evidence of a chemical degradation during the ultrasound injection of PA12 material since the same peaks remains in all the tested samples and no new absorption peaks are observed.

Table 4 shows the molecular weights along the defined sample regions. For comparison, the *Mw* of the raw material is also listed. It can be observed that the *Mw* varies along the formed samples. In fact, the sample center has the lowest *Mw* value when compare to the raw PA12 pellets material and to the other sample regions. Furthermore, experimental results show that the variation in *Mw* is accompanied by a variation of the polydispersity index (PDI) along the sample region. Therefore, it can be said that the evolution of the *Mw* appears to be due to physical than to chemical effects. In fact, the evolution of the *Mw* along the sample regions could be attributed to chain scission events [20,22].

Fig. 9 presents SWAXS measurements at the three defined regions of a sample processed with an applied pressure of 4 bar and 5 s of vibration time considering patterns at 0° and 90°. Measurements indicate that the end sample region differs from the injection and center regions, and the measured patterns presented different absorption. This deviation can be attributed to an alignment of PA12 chains since this region is located at the end of the mold cavity. Therefore, it can be said that the chain alignment is mostly due to the polymer formability at the die exit during the injection process.

Microscope images at the injection and end regions of the specimens evidenced that the material was more homogeneous at the end region, as it can be observed in Fig. 9. From the middle of the sample until the end, a lineal flow was achieved, resulting in better appearance. This occurs because the amount of energy applied to the polymer to melt it, which generates turbulences into the melt, and the short distance

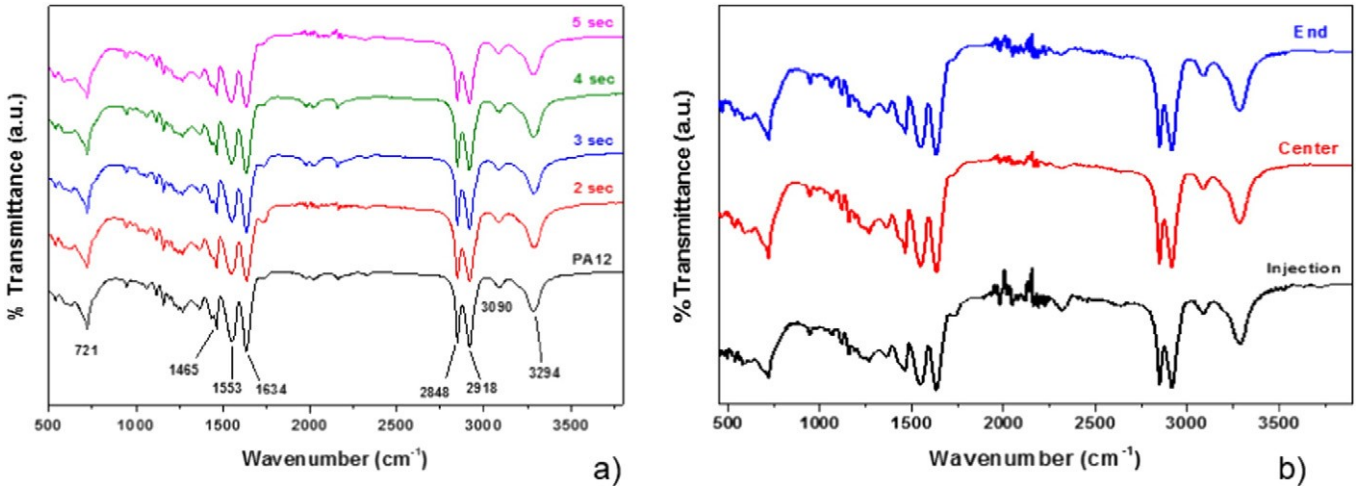

Fig. 8. ATR-FTIR spectra of a) Parts obtained at 4 bar and 2, 3, 4 and 5 s of vibration time; b) FTIR spectra PA12 samples manufactured at 4 bar and 5 s of vibration time at three different regions.

Table 4
Molecular weight of PA12 material.

Sample	Mw ($\times 10^4$)	PDI
PA12 pellets	7.03	1.96
Injection region	6.54	2.07
Center region	6.43	2.02
End region	7.05	1.89

from the plasticization chamber to the molded part (2 mm), which is not large enough to homogenize the melt flow. Flow and sink marks can be detected at the beginning of the parts. This defects can be caused by low temperature values, velocity and injection pressure. For this reason, parts processed with lower ultrasonic time and pressure tend to have more defects.

4.5. Energy flow analysis

This section analyzes the energy dissipated by the process according the variation of the process parameters and compares it to the energy required to melt the material. Fig. 10a shows the energy supplied by the ultrasonic generator to process 300 mg of polyamide with different processing parameters after each cycle. As can be observed, the supplied energy tends to reduce when increasing the applied pressure and increase when the ultrasonic time increase too. The lower the pressure is, more energy has to provide the generator to carry out the melting cycle whereas the delivered energy drops significantly at higher pressure. As expected, the length of vibration time increases the amount of energy supplied keeping the polymer melt more time and assuring the cavity filling.

Next, the comparison between the theoretic power dissipated by the sonotrode (Eq. 16) and the average power required to melt the studied amount of material (Eq. 17) is presented in Fig. 10b. The sonotrode dissipated power is pressure dependent, therefore this power is higher when the pressure increases. The polymer melting energy is plotted according to vibration time, shown by the horizontal lines at 1 s, 2 s, and 4 s of vibration on Fig. 10b. In this case the values considered for the C_p and ΔH_f were 2.10 J/gK and 245 J/g. Thus when the time is higher, less power is required for melting the same amount of material.

Fig. 10b shows that when the energy dissipated by the sonotrode is lower, more energy from the generator is required to complete the process, while for higher values of pressure applied, the energy consumption decreases. This could indicate that the higher the pressure is, the better the utilization of the energy for melting the polymer. Thus, the

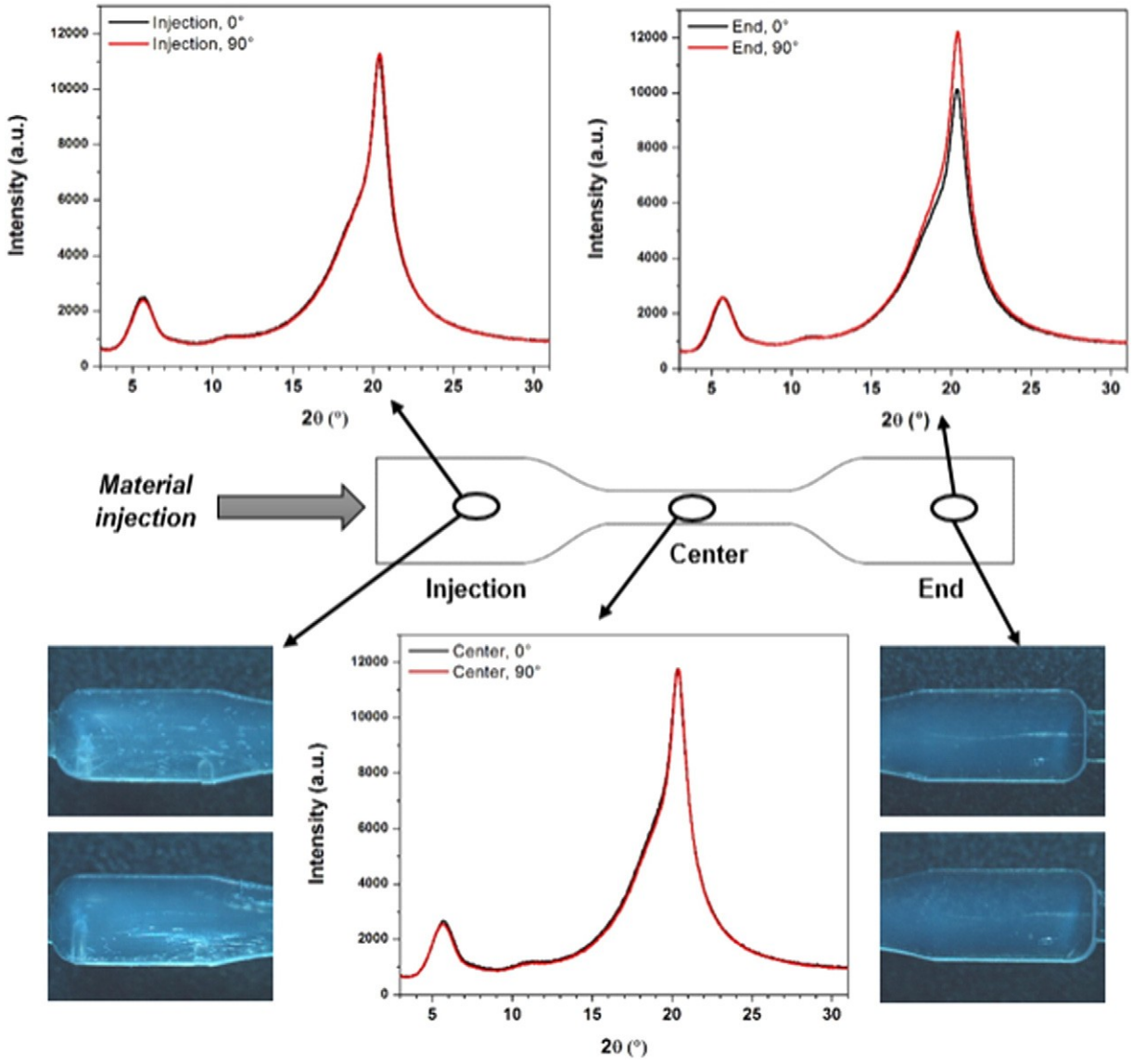

Fig. 9. SWAXS measurements collected in PA12 sample at the injection, center, and end regions by considering patterns at 0° and 90°.

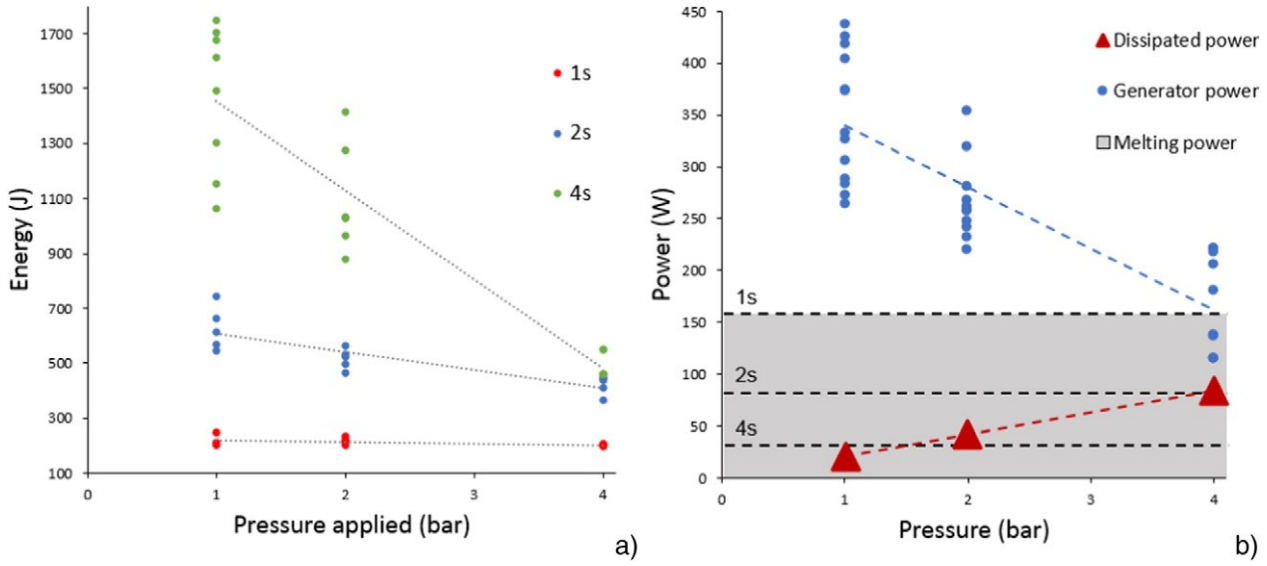

Fig. 10. a) Measured ultrasonic generator energy, and b) Comparison between generator, dissipated and required average power.

process efficiency varies from around 10% at lower pressures to 50% at higher pressures. In any case, the generator's maximum power of 1500 W is achieved.

Moreover, results also indicates that the power delivered by the sonotrode is lower than the power required to melt the material in 1 s, which explains why it was not possible to obtain completed parts with such vibration time. By increasing the cycle time, the required average power decreases and completed specimens can be obtained. Although this analysis is based on a theoretical approach, the obtained results are in accordance with the experimental observation.

When comparing the process's efficiency with other conventional processes, about 20% of the total energy involved in the injection process goes into heating the plasticizing unit [28] and according to Spiering et al. [29], energy consumption in injection molding is around 40%, including the mold movements, heating and the injection process. However, both authors stated that the energy efficiency of injection processes is closely related to the type and quantity of the material, processing time, where fine mold process parameters are essential, and the type of energy generator i.e. electric, hydraulic or hybrid. Electric generators are in fact the most efficient. The ultrasonic molding machine used in this study is electro-pneumatic and the quantity of the scrap is somewhat reduced at less than 10% of the final part.

5. Conclusions

In ultrasonic molding, the combination of vibration amplitude, pressure applied and vibration time determines the amount of ultrasonic energy that is transferred to the polymer, resulting in different amounts of polymer melt which are forced to fill a mold to obtain the final part. This research demonstrates that these parameters directly affect cavity filling, part accuracy, mechanical properties and homogeneity. However, a relationship between those parameters has to be found in order to guarantee pellet plasticization and avoid material degradation. The experimentation presented proves that 300 mg of polyamide pellets can be melted and injected to manufacture small specimens in ultrasonic molding. In addition, it has been found through the energy balance that the acoustic energy provided by the sonotrode and the generator are closely related to the experimental collected data. This can give information of how the process parameters must be adjusted in order to increase the ultrasound process efficiency.

As this is such a new technology, the processing parameters with which to manufacture parts from different materials are still unknown. In conventional techniques, raw material suppliers provide the recommended processing conditions, usually in terms or temperatures and pressure, to avoid the raw material's degradation. In the particular case of ultrasonic molding, material temperature is not directly controlled, and, until now, there has been no accurate relationship between the temperatures reached by the polymer as a consequence of the processing parameters. In this regard, in this paper, a preliminary approach is obtained, and it can be expected that more energy should be applied to materials with higher melting temperatures. However, other parameters such as absorption of the vibration of each material as well as the raw material's shape and the amount of melt to be produced could also influence the processing conditions and the final material properties.

In general, better results are obtained when the processing parameters are increased. Filling rate, dimensional accuracy, part homogeneity and yield strength are positively affected when ultrasonic time and pressure applied are increased. However, maximum values for each of them can be found in order to avoid material degradation and maintain the process performance.

The parts obtained presented good replicability of mold geometry, achieving a minimum deviation of 2 μm from the target value, and around 99% accuracy is observed in the studied zones. Tension tests of the samples obtained presented values of yield strength similar to the expected values for injection molding. Strain values are higher than the reported ones, but they could have been affected by the scaling of the specimen.

Furthermore, the material characterization by using the experimental techniques such as FTIR, GPC, and SWAXS show that there in not chemical degradation on the polymer material due to the ultrasonic injection process. However, the molecular weight variation along the specimen shows that there is mechanical material degradation because of the chain scissions induced by polymer shear stresses. Moreover, there is evidence of chain alignment mostly attributed to the material flow into the die mold cavity.

Future work should be focused on comparing ultrasonic molding and injection molding, maintaining the mold geometry and processing conditions such as cooling time, packing pressure, cooling ratio, in order to make a comparison between the parts obtained when using those technologies.

Acknowledgments

The authors would like to express their gratitude to Eurecat Technology Center and Ultrasion SL for their support and assistance. The project was carried out under the DPI2013-45201-P reference grant awarded

by the Spanish Government and with the financial support from the University of Girona (Spain) MPCUdG2016/036, and to the Consejo Nacional de Ciencia y Tecnología de México (CONACYT), Project Number 242269. The authors also acknowledge Marcelo Lozano for helping us in the material characterization by performing the FTIR, GPC, and SWAXS specimens experimental analysis.

References

[1] V. Bellantone, R. Surace, G. Trotta, I. Fassi, Replication capability of micro injection moulding process for polymeric parts manufacturing, Int. J. Adv. Manuf. Technol. 67 (2012) 1407–1421, http://dx.doi.org/10.1007/s00170-012-4577-2.

[2] U.M. Attia, J.R. Alcock, An evaluation of process-parameter and part-geometry effects on the quality of filling in micro-injection moulding, Microsyst. Technol. 15 (2009) 1861–1872, http://dx.doi.org/10.1007/s00542-009-0923-1.

[3] N. Zhang, M.D. Gilchrist, Characterization of microinjection molding process for milligram polymer microparts, Polym. Eng. Sci. (2013) 1–13, http://dx.doi.org/10.1002/pen.23677.

[4] J. Giboz, T. Copponnex, P. Mélé, Microinjection molding of thermoplastic polymers: a review, J. Micromechanics Microengineering. 17 (2007) R96–R109, http://dx.doi.org/10.1088/0960-1317/17/6/R02.

[5] W. Michaeli, T. Kamps, C. Hopmann, Manufacturing of polymer micro parts by ultrasonic plasticization and direct injection, Microsyst. Technol. 17 (2011) 243–249, http://dx.doi.org/10.1007/s00542-011-1236-8.

[6] J. Grabalosa, I. Ferrer, O. Martínez-Romero, A. Elías-Zúñiga, X. Plantá, F. Rivillas, Assessing a stepped sonotrode in ultrasonic molding technology, J. Mater. Process. Technol. 229 (2016) 687–696, http://dx.doi.org/10.1016/j.jmatprotec.2015.10.023.

[7] W. Michaeli, A. Spennemann, R. Gärtner, New plastification concepts for micro injection moulding, Microsyst. Technol. 8 (2002) 55–57, http://dx.doi.org/10.1007/s00542-001-0143-9.

[8] W. Michaeli, D. Opfermann, Ultrasonic plasticising for micro injection moulding, in: W. Menz, S. Dimov (Eds.),Multi-Material Micro Manuf., Grenoble 2006, pp. 345–348.

[9] W. Michaeli, T. Kamps, Heating and plasticizing thermoplastics with ultrasound for micro injection molding, Annu. Tech. Conf. - ANTEC, Conf. Proc. 2010, pp. 323–327.

[10] B. Jiang, J. Hu, J. Li, X. Liu, Ultrasonic Plastification Speed of Polymer and its Influencing Factors, (2012), 2010–2013, http://dx.doi.org/10.1007/s11771.

[11] M. Sacristán, X. Plantá, M. Morell, J. Puiggalí, Effects of ultrasonic vibration on the micro-molding processing of polylactide, Ultrason. Sonochem. 21 (2014) 376–386, http://dx.doi.org/10.1016/j.ultsonch.2013.07.007.

[12] M. Planellas, M. Sacristán, L. Rey, C. Olmo, J. Aymamí, M.T. Casas, et al., Micromolding with ultrasonic vibration energy: new method to disperse nanoclays in polymer matrices, Ultrason. Sonochem. 21 (2014) 1557–1569, http://dx.doi.org/10.1016/j.ultsonch.2013.12.027.

[13] P. Negre, J. Grabalosa, I. Ferrer, J. Ciurana, A. Elías-Zúñiga, F. Rivillas, Study of the ultrasonic molding process parameters for manufacturing polypropylene parts, Procedia Eng. 132 (2015) 7–14, http://dx.doi.org/10.1016/j.proeng.2015.12.460.

[14] S.W. Rienstra, A. Hirschberg, An Introduction to AcousticsEindhoven 2015, http://dx.doi.org/10.1119/1.1933163.

[15] A. Levy, S. Le Corre, N. Chevaugeon, A. Poitou, A level set based approach for the finite element simulation of a forming process involving multiphysics coupling: ultrasonic welding of thermoplastic composites, Eur. J. Mech. A. Solids. 30 (2011) 501–509, http://dx.doi.org/10.1016/j.euromechsol.2011.03.010.

[16] J. Li, S. Guo, X. Li, Degradation kinetics of polystyrene and EPDM melts under ultrasonic irradiation, Polym. Degrad. Stab. 89 (2005) 6–14, http://dx.doi.org/10.1016/j.polymdegradstab.2004.12.017.

[17] J. Chen, Y. Chen, H. Li, S.-Y. Lai, J. Jow, Physical and chemical effects of ultrasound vibration on polymer melt in extrusion, Ultrason. Sonochem. 17 (2010) 66–71, http://dx.doi.org/10.1016/j.ultsonch.2009.05.005.

[18] J. Lee, N. Kim, Investigation of the numerical analysis for the ultrasonic vibration in the injection molding, Korea-Australia Rheol. J. (2009).

[19] M.M. Caruso, D.A. Davis, Q. Shen, S.A. Odom, N.R. Sottos, S.R. White, et al., Mechanically-induced chemical changes in polymeric materials, Chem. Rev. 109 (2009) 5755–5798, http://dx.doi.org/10.1021/cr9001353.

[20] J. Li, M. Liang, S. Guo, Y. Lin, Studies on chain scission and extension of polyamide 6 melt in the presence of ultrasonic irradiation, Polym. Degrad. Stab. 86 (2004) 323–329, http://dx.doi.org/10.1016/j.polymdegradstab.2004.04.021.

[21] M. Vazquez, D. Schmalzing, P. Matsudaira, D. Ehrlich, G. McKinley, Shear-induced degradation of linear polyacrylamide solutions during pre-electrophoretic loading, Anal. Chem. 73 (2001) 3035–3044, http://dx.doi.org/10.1021/ac001294+.

[22] B.A. Buchholz, J.M. Zahn, M. Kenward, G.W. Slater, A.E. Barron, Flow-induced chain scission as a physical route to narrowly distributed, high molar mass polymers, Polymer (Guildf) 45 (2004) 1223–1234, http://dx.doi.org/10.1016/j.polymer.2003.11.051.

[23] A. Levy, S. Le Corre, I. Fernandez Villegas, Modeling of the heating phenomena in ultrasonic welding of thermoplastic composites with flat energy directors, J. Mater. Process. Technol. 214 (2014) 1361–1371, http://dx.doi.org/10.1016/j.jmatprotec.2014.02.009.

[24] M. Kurt, O. Saban Kamber, Y. Kaynak, G. Atakok, O. Girit, Experimental investigation of plastic injection molding: assessment of the effects of cavity pressure and mold temperature on the quality of the final products, Mater. Des. 30 (2009) 3217–3224, http://dx.doi.org/10.1016/j.matdes.2009.01.004.

[25] C. Yang, X.-H. Yin, G.-M. Cheng, Microinjection molding of microsystem components: new aspects in improving performance, J. Micromechanics Microengineering. 23 (2013) 093001, http://dx.doi.org/10.1088/0960-1317/23/9/093001.

[26] P. Xie, F. Guo, Z. Jiao, Y. Ding, W. Yang, Effect of gate size on the melt filling behavior and residual stress of injection molded parts, Mater. Des. 53 (2014) 366–372, http://dx.doi.org/10.1016/j.matdes.2013.06.071.

[27] S. Meister, D. Drummer, Influence of manufacturing conditions on measurement of mechanical material properties on thermoplastic micro tensile bars, Polym. Test. 32 (2013) 432–437, http://dx.doi.org/10.1016/j.polymertesting.2012.12.006.

[28] D. Godec, M. Rujnic-Sokele, M. Šercer, Processing parameters influencing energy efficient injection moulding of plastics and rubbers, Polimeri. 33 (2012) 112–117.

[29] T. Spiering, S. Kohlitz, H. Sundmaeker, C. Herrmann, Energy efficiency benchmarking for injection moulding processes, Robot. Comput. Integr. Manuf. 36 (2015) 45–59.